室蘭工業大学
学術資源アーカイブ
Muroran Institute of Technology Academic Resources Archive

A study on shelter airport selection during large-scale volcanic disasters using CARATS open dataset

メタデータ	言語: eng 出版者: PERGAMON-ELSEVIER SCIENCE LTD 公開日: 2022-03-23 キーワード (Ja): キーワード (En): Genetic algorithm, Large-scale volcanic disasters, Shelter airport selection 作成者: Arreeras, Saharat, Arimura, Mikiharu メールアドレス: 所属:
URL	http://hdl.handle.net/10258/00010465

Transportation Research Part C 129 (2021) 103263

Contents lists available at ScienceDirect

Transportation Research Part C

journal homepage: www.elsevier.com/locate/trc

A study on shelter airport selection during large-scale volcanic disasters using CARATS open dataset

Saharat Arreeras, Mikiharu Arimura *

Division of Sustainable and Environmental Engineering, Muroran Institute of Technology, Muroran 050-8585, Japan

ARTICLE INFO

Keywords:
Genetic algorithm
Large-scale volcanic disasters
Shelter airport selection

ABSTRACT

Air transport supports economic growth and prosperity through the movement of passengers and goods. As it grows more extensive and more complex, the more vulnerable its operations to unexpected natural disasters (e.g., typhoon and volcanic eruption) will become. In Japan, many active volcanos are affecting its airspace and considered a threat to the national air transportation and critical aviation equipment such as aircraft. The study focuses on solving the evacuation of the affected aircraft during the volcanic eruption by proposed the shelter airport selection model using the historical data of volcanic eruption, aircraft movement, and airports data in Japan. The model was applied to the genetic algorithm (GA), the metaheuristic algorithm to provide the approximate solution of the suitable shelter airport with minimum flight time and no exceeded shelter airports' capacities for the aircraft evacuation.

1. Introduction and background

Airports are the critical aviation infrastructure and essential to their regions' economic activities and even more critical during the disaster (Smith, 2010) such as earthquakes, volcanic eruptions, and human-made disasters. Recently, the airline industry had encountered the uncertain situations of volcanic eruption and its ash cloud when the Eyjafefjallajökull and Merapi Volcano erupted in 2010, which had significantly disrupted air transport and economy in Europe and Indonesia's central (Langmann et al., 2012; Mazzocchi et al., 2010; Picquout et al., 2013). In Japan, the volcanic eruption is one of the national air transportation threats as there are more than 100 active volcanos, and many of them are located in the busy airspace and large hub/regional airports. Although the safety operation regulations during the volcanic eruption have been established by ICAO and Japan Meteorological Agency (JMA), there is no shelter airport selection system with integrated air flight and airport data available, which is considered as a problem in this study. Therefore, we aim to develop a shelter airport selection model for the event of a volcanic eruption.

In the disaster times, the surrounding unaffected airports are expected to quickly respond and fulfill the affected airports' loss capacity to reduce the disaster's wide-effect (Button et al., 2010; Hanaoka et al., 2013). The Japan catastrophic earthquake in March 2011 caused the loss of Sendai international airport, one of the major air transportation hubs in East Japan. Other regional and smaller local airports' role became more important on bypassing, maintaining the connections between remaining airports, and securing the unoperated equipment included aircraft (Cidell, 2006; Kita et al., 2005). These unforeseeable conditions can reduce the level of airport operation performance, create air traffic congestion, and put pressure on airport resources from limited resource utilization (Harsha, 2003).

* Corresponding author.
E-mail addresses: 19096002@mmm.muroran-it.ac.jp (S. Arreeras), arimura@mmm.muroran-it.ac.jp (M. Arimura).

https://doi.org/10.1016/j.trc.2021.103263
Received 5 March 2020; Received in revised form 28 April 2021; Accepted 7 June 2021
Available online 2 July 2021
0968-090X/© 2021 The Authors. Published by Elsevier Ltd. This is an open access article under the CC BY-NC-ND license (http://creativecommons.org/licenses/by-nc-nd/4.0/).

The airport's practical resource utilization could be achieved by integrating various operations, including aircraft maintenance, flight operations, ground handling, fueling services, airside services, and air traffic control (Harriman et al., 2009). Madas and Zografos studied airport slot allocation under the situation of air traffic congestion by airport's classification, capacity and size, and air traffic demand to measure the airport handling capability before choosing the suitable slot allocation for aircraft (Madas and Zografos, 2010). The other studies showed that airport capacity had a significant impact on aircraft and passenger relocation in the event of disruptions, which was also mentioned in other studies concerning airport slot allocation problems (Hu et al., 2016; Lordan et al., 2015, 2014; Lordan and Klophaus, 2017). Hence, the large airports (hub and regional airports) are expected to become emergency airports in surging air traffic demands during the disaster from their operations and capacities readiness.

Airport disaster management (ADM) studies have put the focusing on the airport resources capacity utilization on both landside and airside, which airside capacity is defined into three parts: runway(s), taxiway(s), and apron area (the aircraft stands area for loading, unloading, and refueling) within the airport capacity constraints (Jimenez Serrano and Kazda, 2017). In particular, the aircraft stands allocation (SA) for accommodating the affected aircraft but rarely the study on SA during the disaster. Instead, a bundle of studies on airport gate assignment problem (AGAP) is available. Most of them had set on the four main minimization objectives, i.e., the passenger's walking distance, the number of ungated flights, dispersion of idle gate periods, passenger travel time, and the number of flights exceeds the number of available gates. Many studies had applied various *meta*-heuristic algorithms to solve these optimization problems on aircraft stand allocation and proved to be necessary to solve such NP-hardness of the optimization problem as SA (Guépet et al., 2015). Those applied *meta*-heuristic algorithms included simulated annealing (Cheng et al., 2012; Ding et al., 2005), bee colony optimization (Dell'Orco et al., 2017; Marinelli et al., 2015), tabu search, and genetic algorithm (Aktel et al., 2017; Cheng et al., 2012; Ding et al., 2005; Liu and Kozan, 2016; Marinelli et al., 2015). Although the studies mentioned above did not intend to solve airport selection and aircraft assignment during the disaster. However, they had given a big picture of the concerning factors on airport disaster management, resource utilization, and optimization algorithms, which can develop the computational optimization model on shelter airport selection for aircraft evacuation during the natural disaster.

In principle, the optimization model for shelter location selection was built for large-scale emergencies to select shelters from the exited safe and suitable locations according to both evacuee and shelter location criteria. The main goals are responsiveness and cost-efficiency by minimizing total evacuation cost, time, and the entire transport distance between demand points (an affected area and candidate facilities). Regularly, the evacuation is evaluated its efficiency by distance or time (Toregas et al., 1971). Thus, the first objective function aims to focus on the travel distance and time criterion. The minimization of total or minisum formulation had widely applied to the optimization models on the facility selection of humanitarian relief supply distribution in the various natural disasters, i.e., hurricane and earthquake (Horner and Downs, 2010; Lin et al., 2012). The metaheuristic approach, such as the genetic algorithm (GA), has recently introduced to the complex multi-criteria objective optimization problems of optimal shelter selection on the flooding evacuation planning, earthquake shelter location selection, and the facility location selection in response to large-scale emergencies (Hu et al., 2014; Kongsomsaksakul et al., 2005).

Therefore, this study aims to propose an airport selection model for aircrafts evacuation in a volcanic eruption situation by considering the airport's available aircraft stands capacity, aircraft size, and enclosed area to avoid volcanic ash cloud. The proposed model has been developed and applied to the genetic algorithm (GA), then analyzed its performance according to the study's objective and subject. The study also compared GA's performance with the Greedy Randomized Adaptive Search Procedure (GRASP), the basic multi-start *meta*-heuristic algorithm on the same developed model. Although GRASP does not equip with the crossover and mutation operators like in GA. GRASP has a similar mechanism to GA in its ability to randomly generate initial solutions, evaluate, select the better solution, and replace it with a better new local optimal solution in each iteration. Even though both GA and GRASP may or may not promise the global-optimal results, their procedures could ensure that the best result or approximate results will be generated at the end of all running iterations. Therefore, their results could suggest aviation authorities and related parties, e.g., air traffic control agencies, airports, and airlines, on which airport could be the critical shelter airports for aircraft evacuation of the volcanic eruption minimize effected of the event.

This paper's remainder is organized as follows: Section 2 presents the methodology, dataset, and proposed mathematical model of research. The case study of Mt.Hakone is presented in Section 3 with models' validations in Section 4 and computational results in Section 5. Finally, the conclusion, future research suggestions, and research limitations are presented at the end of the study.

2. Methods and materials

This section discusses a conceptual model and assumption, Genetic algorithm (GA) and Greedy Randomized Adaptive Search Procedure (GRASP), the collaborative actions for the renovation of air traffic systems (CARATS) flight dataset, and the proposed mathematical model and its pseudocodes as follows:

2.1. Genetic algorithm (GA) and Greedy Randomized Adaptive Search Procedure (GRASP)

Genetic Algorithm (GA) is a type of evaluation algorithm. Darwin's theory of evolution is an optimization method based on concepts of natural selection and genetics. They work with individuals' populations; each evolves by adapting itself to the

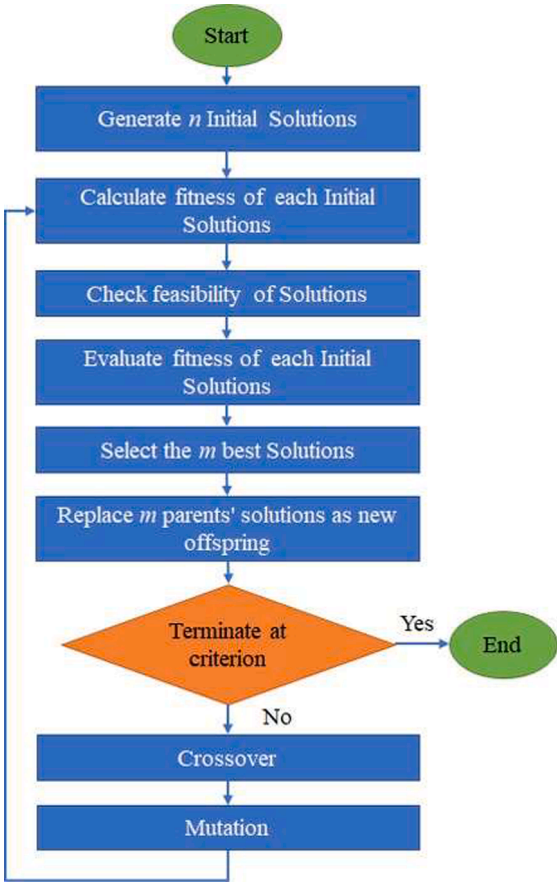

Fig. 1. The process flow of the Genetic Algorithm (GA).

environment, repeating crossover, mutation, and selecting a possible solution to a given environment's conditions or problem. The appropriate solution can be found by using the series of numerical computation. GA typically works by iteratively generating and evaluating individuals using an evaluation function. The basic process flow of GA is shown in Fig. 1.

The performance of the model applied on GA is compared with the basic *meta*-heuristic algorithm, Greedy Randomized Adaptive Search Procedure (GRASP). GRASP is the basic multi-start *meta*-heuristic algorithm for combinatorial optimization problems proposed by Feo and Resende in 1995 (Feo and Resende, 1995). In each running iteration of the GRASP algorithm consists of two steps: construction and local search. In the construction step, a feasible candidate solution is built using randomized greedy heuristic. The second step, the solution is used as the initial solution for the local search procedure. If an improved solution is found in the local search, the best candidates or *restricted candidate list* (RCL) will be replaced by the better one (see Fig. 2.).

Moreover, the study adopted the haversine formula for distance and flight time calculation. Since the study's distance is the geodesics or curve line between two points on earth's surface using Latitude and Longitude of given aircraft I and shelter airport J set. The flight time of any affected aircrafts took from their current position to the safe shelter airports was calculated by flying distance divided average cruising speed of commercial aircraft at 880 km/h. It helps to measure the solution's performance, so-called *fitness* value for both algorithms. When termination criterion is met, such as the maximum number of iterations or the optimal solution has been found, the algorithm will be terminated and return the best solution.

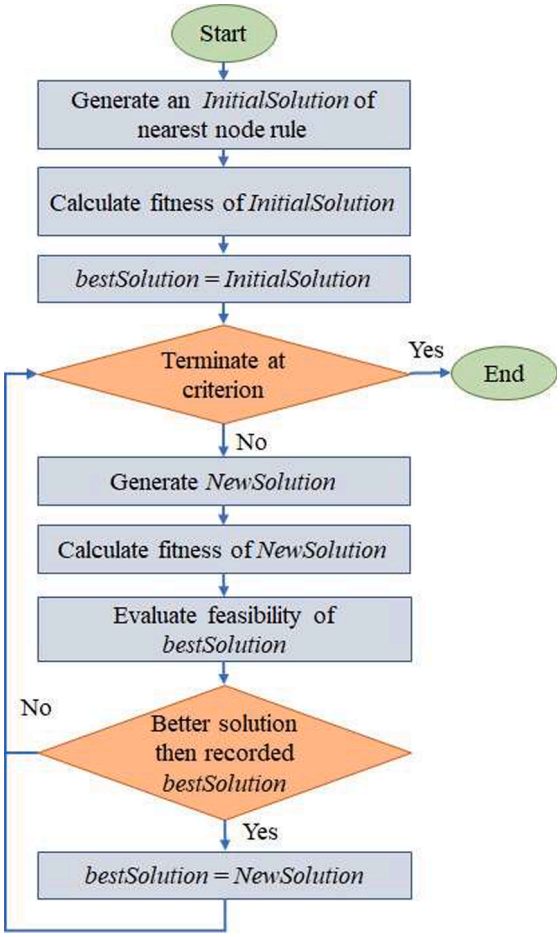

Fig. 2. The process flow of the Greedy Randomized Adaptive Search Procedure (GRASP).

2.2. *The collaborative actions for renovation of air traffic systems (CARATS) flight dataset*

The Collaborative Actions for Renovation of Air Traffic Systems (CARATS) dataset is a historical flight record cover all Japan's area control centers; Sapporo, Tokyo, and Fukuoka Area Control Center (ACC), consist of raw flight data of individual aircraft, i.e., date, timestamp of 10sec interval, latitude, longitude, altitude, and model of aircraft (e.g., B777 and A322) provided by Japan MLIT (MLIT, 2018) as shown in Table 1.

Table 1
Example of CARATS flight dataset provided by Japan MLIT.

Time	Flight_ no.	Latitude	Longitude	Altitude	AC_type	Latitude	Longitude
00:03.9	FLT1861	27.420048	124.383047	38,000	B77W	27°25′12.17	124°22′58.97
00:13.9	FLT1861	27.408566	124.369262	38,000	B77W	27°24′30.84	124°22′09.34
00:23.9	FLT1861	27.396312	124.353317	38,000	B77W	27°23′46.72	124°21′11.94
00:33.9	FLT1861	27.384821	124.339389	38,000	B77W	27°23′05.36	124°20′21.80
00:43.9	FLT1861	27.373473	124.326036	38,000	B77W	27°22′24.50	124°19′33.73

2.3. Proposed models

The Computational model for genetic algorithm (GA) and Greedy Randomized Adaptive Search Procedure (GRASP) is proposed for shelter airport selection and evacuation planning. The developed models' objective is to minimize the total flight time of aircrafts taken from their current position to safe shelter airports. The models had considered the limitation of shelter airport accommodation capacity by the number of available aircraft stands and their sizes, and the affected aircraft sizes. The assumptions of the problem on model construction, indices, parameters, decision variables, objective function, constraints, genetic algorithm's operators, including GA and GRASP pseudocodes in Algorithm 1 and Algorithm 2, are described as follows:

Algorithm 1. (*Proposed model pseudocode for Genetic Algorithm (GA)*)

Input: J, a set of candidate airport locations; M, a set of candidate airport locations capacity; and I, a set of affected aircraft locations;
Output: A list of the nearest X_j selected shelter airports for each E_{ij} affected aircraft;
Initialize Populations: 500 solutions of all affected aircraft $i \in I$ with 42 random candidate airports $j \in J$ as candidate solutions.
Evaluate each solution's fitness using the minimum total flight of the solution **do**
  compute flight time, the distances between each affected aircraft $i \in I$ and all candidate shelter airport $j \in J$; using haversine formula;
Repeat Until termination condition is satisfied; 500 iterations **do**
  Select parents; 3 solutions parents
  Crossover pairs of parents using two-points crossover operator;
  Mutate the offspring using the mutUniformInt operator to change the solution's value randomly;
  Evaluate each solution's fitness using the minimum total flight of the solution **do**
    compute flight time from the distances between i and all $j \in J$ for each population E_{ij};
    Foreach $E_{ij,}$ aircraft i to candidate airport j **do**
      check sum of assigned aircraft at shelter airport j; $\sum_j E_{ij}$, compare to NC_j, the available stands and stands' sizes at airport j;
      if $\sum_j E_{ij} \leq NC_{j;}$ exit;
else then
compute add additional flight time (penalty) according to number of exceeded aircraft at airport j to the solution;
$h_j = |a^*(\sum_{i \in I} E_{ij} - NC_j)|$; exit;
    End for
  Select the 3 best solutions: minimum fitness by total flight time
  Store the results in a list of selected airports
  Add the new best solution to the population list for the next iteration
Terminate

Algorithm 2. (*Model pseudocode with limited airport capacity constraint for Greedy Randomized Adaptive Search Procedure (GRASP)*)

Input: J, a set of candidate airport locations; M, a set of candidate airport locations capacity; and I, a set of affected aircraft locations;
Output: A list of the nearest selected shelter airports X_j for each E_{ij} affected aircrafts;
Initialize Solution: a set of all affected aircraft $i \in I$ population with 42 random candidate airports $j \in J$ as candidate solutions. **the total number of selected candidate airports in each population set must not exceed maximum handling capacity by aircraft size of each airport; capacity by aircraft size: small, medium, and large.
  Foreach affected aircraft $i \in I$ **do**
    compute flight time, the distances between each affected aircraft $i \in I$ and all candidate shelter airport $j \in J$; using great-circle distance;
    sort the computed flight time, smallest to largest;
    select the nearest airport by the shortest flight time;
    Foreach affected aircraft i to candidate airport j **do**
     check sum of assigned aircraft at shelter airport j; $\sum_j E_{ij}$, compare to NC_j, the available stands and stands' sizes at airport j;
        if $\sum_j E_{ij} < NC_j$then
        assign aircraft i to the candidate shelter airport j; exit;
        else then
        select the new next nearest shelter airport $j + 1$;
    End for
  End for
Evaluate a solution's fitness using minimum total flight time of the solution **do**
Store the results in a list of selected airports if fitness value better than min(fitness) of all previous solution in the list
Repeat Until termination condition is satisfied;*500* iterations **do**
  Generate a new solution by randomly select airports with distance and capacity constraints the same as items 1–15
Terminate

2.3.1. The assumptions of the problem on model construction

According to ICAO's volcanic ash effect on aircraft engine's performance, all aircraft must avoid contact with volcanic ash particles and rocks by flying into or park inside the volcanic eruption affected areas and airspace in any ash cloud density level. It can be assumed that at any volcanic eruption, warning level has been delivered both airborne and on-ground (*I*) need to avoid those areas by rerouting, rescheduling, or cancel their schedules and evacuate to the safe shelter airports; *J*, at all causes.

1. Since volcanic ash particles can cause severe damage an aircraft's engine, no shelter airport can be located within the affected area; *F*, is allowed.
2. Each shelter airport has limited capacity to accommodate the evacuation demand, the limited number of aircraft handling by sizes of aircraft, and the runway's length. The maximum occupancy rate of aircraft stands (*OCj*) were used to determine the maximum number of occupied stands at the affected airport (considered as the number of affected on-ground aircrafts), and available stands at the shelter airports. The occupancy rate can be calculated using; the maximum cumulative number of arrival and departure flights in one hour during the busiest day of the airport and its maximum number of aircraft stands.
3. The aircrafts assignment to available aircraft stands will be in sequential according to their size and available stands by aircraft sizes at the shelter airport. Each aircraft size: small, medium, large, and extra-large aircraft has its specific handling equipment and size defined by ICAO. Even though all available aircraft stand can accommodate various sizes and types of aircraft, selecting the most appropriate one will cost the airport less to accommodate those aircrafts in an emergency. Each airport also has its specific aircraft handling capacity by which size of aircraft it could handle by wingspan (ICAO, 2019, 2016). See detail of runway length by aircraft wingspan detail in Table A5. Hence, an affected aircraft will be assigned to an aircraft stand that matched its size as a primary assignment, i.e., a small aircraft to a small-size stand, a medium-size aircraft to a medium-large size stand, a large and extra-large size aircraft to a large size stand. If the size-matched stand is fully occupied, an aircraft could be assigned to the next larger size stand, i.e., a small-size aircraft to a medium-large size stand. The sequence of aircraft stands assignment for each aircraft's sizes is shown in Fig. 3.

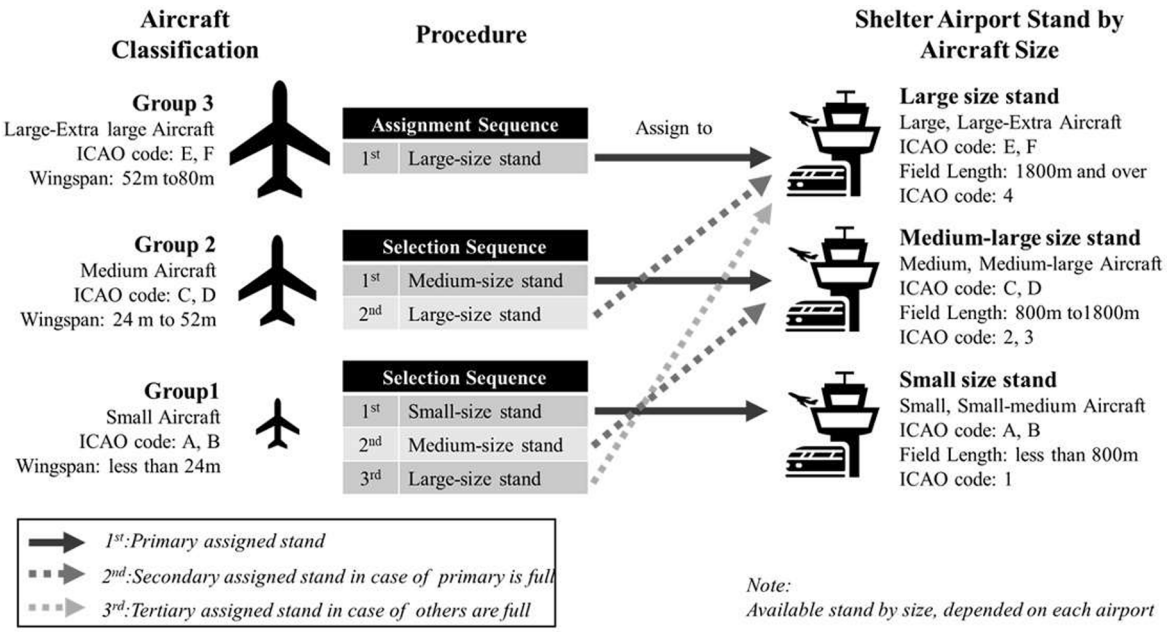

Fig. 3. The sequence of aircraft stands assignment for each aircraft's sizes matching, airport available aircraft stands, and field (runway) length.

Index sets	
I	Set of affected aircrafts; $i \in I$
J	Set of candidates shelter airports; $j \in J$
S	Set of affected aircraft sizes; $s \in \xi$, associated with I
F	Set of affected airports; $f \in F$
Parameters	
M_j	Maximum number of aircraft stands of selected shelter airport; $j \in J$
D_{ij}	Distance (km) from the current position of affected aircrafts $i \in I$, to shelter airport $j \in J$
OC_j	Occupancy rate of the aircraft stands' maximum number M_j at candidate shelter airports $j \in J$
NC_j	Non-occupancy rate of the aircraft stands' maximum number M_j at candidate shelter airports $j \in J$
$P(\rho)_j$	Available medium-size aircraft stands, at shelter airport $j \in J$
$P(\tau)_j$	Available large-size aircraft stands, at shelter airport $j \in J$
ρ_{sj}	Equal to 1 if a medium-size aircraft $s \in \xi$ been assigned to a medium or large-size aircraft stand at shelter airport $j \in J$, 0 otherwise.
τ_{sj}	Equal to 1 if a large-size aircraft $s \in \xi$ been assigned to a large-sized aircraft stand at shelter airport $j \in J$, 0 otherwise.
ς_{sj}	Equal to 1 if a small-size aircraft $s \in \xi$ been assigned to any stand at shelter airport $j \in J$, 0 otherwise.
h_j	Penalty value or additional flight time (hr) value gives a candidate shelter airport $j \in J$ according to the number of aircraft $i \in I$, which has been exceeded assign from the airport's available capacity.
t_{ij}	Flight time (h) of each affected aircraft $i \in I$ to shelter airport $j \in J$; $t_{ij} = D_{ij}\tilde{\text{A}} \cdot 880(km/hr)$
Decision variables	
X_j	Equal to 1 if the selected shelter airport$j \in J$ is in the affected airports $f \in F$, 0 otherwise.
E_{ij}	Equal to 1 if assigned aircraft $i \in I$ to shelter airport $j \in J$ with the correct size of stand, 0 otherwise.
T	Total flight time of all assigned aircrafts $i \in I$.

Objective function

Minimize total flight time of all affected aircrafts $i \in I$ to safe shelter airports $j \in J$

$$minT = \sum_j \sum_i t_{ij} + h_j \forall i, j \tag{1}$$

Subjective to

Evacuate to the airport in the safe zone: selected shelter airport must not be located in the affected area, or the affected airport set F.

$$X_j \notin F \forall j \tag{2a}$$

$$\sum_{j \in J} X_j = 0 \forall j \tag{2b}$$

Candidate shelter airport capacity limitation by aircraft stand sizes: according to aircraft assignment by sizes in Section 2.3.1 and Fig. 3, each affected aircraft could be assigned to the same or larger sizes of the stand to its size. The aircraft stand size constraint has focused on the medium and large aircraft to the smaller size of the aircraft, unlike the small-size aircraft, which could be assigned to any size of available stands as shown in equation (3b) to (3d). However, constraint 3e and 3f states the total number of assigned aircraft of all sizes must not exceed the available or non-occupied aircraft stands (3a); NC_j, of the shelter airport of $j \in J$.

$$NC_j = (1 - OC_j) * M_j \forall j \tag{3a}$$

$$\sum_{s \in \xi} \varsigma_{sj} \leq NC_j \forall j \tag{3b}$$

$$\sum_{s \in \xi} \rho_{sj} \leq P(\rho)_j \vee P(\tau)_j \forall j \tag{3c}$$

$$\sum_{s \in \xi} \tau_{sj} \leq P(\tau)_j \forall j \tag{3d}$$

$$\sum_{i\in I} E_{ij} = \sum_{s\in\xi} \tau_{sj} + \sum_{s\in\xi} \rho_{sj} + \sum_{s\in\xi} \varsigma_{sj} \forall j \tag{3e}$$

$$\sum_{i\in I} E_{ij} \leq NC_j \forall j \tag{3f}$$

2.3.2. Penalty function

In this study, the penalty function has been used to penalize infeasible solutions on the genetic algorithm by disadvantage to its individual's fitness value, force the algorithm to avoid constraint violation. Giving an additional flight time to each violation solution depended on the degree of constraint violation (number of available or non-occupied aircraft stands violation) to control the number of assigned aircraft at shelter airport not to exceed its available capacity. It can be done by assigning constant value h_j to its flight time to disadvantage its fitness according to the degree of constraint violation. Thus, the degree of constraint violation can be calculated from the difference between the total number of assigned aircrafts $\sum_{i\in I} E_{ij}$ at shelter airport $j \in J$ with the correct size of aircraft and stand, and non-occupied aircraft stands NC_j of shelter airport $j \in J$ multiply by constant a where $a \geq 1$ according to ~1 h (65 min) of the average duration on the landing take-off cycle (LTO) and turnaround operations of an aircraft. The LTO cycle contains four operations involved take-off, climb, approach, and taxi with an average duration of 33 min (ICAO, 2013). Moreover, 44 min on average of turnaround time (minimum 29 and maximum 55 min) depend on the size of the aircraft, which included some of these activities; unload and reload its passenger, baggage and cargo, potable and waste-water, and refueling (Airbus, 2005; Costea, 2011; Mota et al., 2017).

$$\delta_j = \sum_{i\in I} E_{ij} - NC_j a \geq 1, \forall j \tag{4a}$$

$$h_j = a^* max(\delta_j, 0) \begin{cases} \delta_j, \delta_j \leq 0 \\ 0, otherwise \end{cases} a \geq 1, \forall j \tag{4b}$$

2.3.3. Genetic algorithm operators

In this study, an evaluation algorithm was based on DEAP, a Python operation framework for evaluation algorithm for primary operators and settings (De Rainville et al., 2012). The value of each operator based on the case study used in this study gives the example of operators' values. However, these values are adjustable to different study cases. The details of GA process flow and sitting are shown in Algorithm 1.

Chromosome encoding: the chromosome N represents a list of destination shelter airports $j \in J$ for all of affected aircraft $i \in I$. Each chromosome consists of I genes, which refer to the number of affected aircrafts I and contain one random number of possible shelter airports $j \in J$. Hence each gene is represented by two elements i and j. For instance, in this study, 261 affected aircrafts needed to evacuate to any 42 possible safe shelter airports. The randomly generated chromosome is shown in Fig. 4. A single chromosome will be consisted of 261 genes.

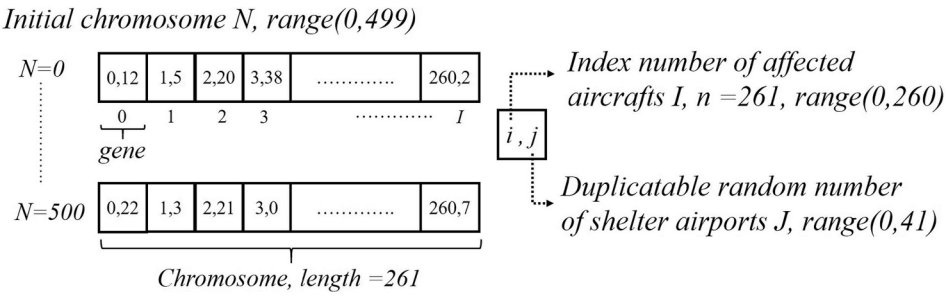

Fig. 4. The GA's chromosome encoding.

Where

I is the number of observable affected aircraft, e.g., 261 aircrafts.
J is the duplicatable number of available shelter airports, e.g., 42 airports.
N is the number of initial chromosome population, e.g., 500 chromosomes.

Initial population: The initial population represents the number of parents' chromosomes at the start point of the algorithms, which equal to or greater than the toursize value as mentioned in the following "Chromosome replacement". The larger number of initial populations could lead to less running iteration for GA to find an approximate solution. However, it could cause a longer calculation duration in each iteration as well. Refer to DEAP: basic setting for the number of initial populations, this study had set the number of initial chromosome population N to 500 chromosomes.

Chromosome evaluation and fitness function: the chromosome was evaluated by the total flight time of every gene calculated using a haversine distance formula divided by average aircraft speed per hour in the form of fitness value. It was also evaluated by the total number of each assigned shelter airport number against the airport's available capacity constraint. For capacity evaluation, the penalty function was used to give the capacity violation genes a disadvantage by giving additional flight time to aircraft if it exceeded-assigned to the airport capacity as defined in Section 2.3.2 penalty method.

Crossover and mutation: the crossover method in this study is based on the two-points crossover operator (cxTwoPoints) (De Rainville et al., 2012), the random gene sequence integer i in I selection to select two crossover positions i within chromosome N and exchange genes between two parents, which reserved original genes values in the chromosome and give diversity to the offspring (child chromosome). Unlike crossover operation, the mutation method used the "mutUniformInt" operator (low $=$ 0, up $=$ 41, inpb $=$ 0.05), which performs an integer replacement between lower and upper bound values probability 5% uniformly, caused the value of gene to change from the original value within the range of the candidate shelter airport J.

Chromosome replacement: the study used the steady-state approach in which the population size remains constant according to the number of initially generated chromosomes. This process was done through the chromosome replacement using the "selTurnament" operator equal to 3, in which the 3 best suitable solutions from offspring replaced the 3 initial parent chromosomes. This process has led to better fitness value on the next generation of offspring in each new running iterations until the GA process was terminated at the end of the setting iteration.

Chromosome decoding: at the termination phase at iteration $=$ 500, the chromosome with the smallest fitness value (the minimum flight time according to objective) is selected as the best chromosome/solution. The chromosome is an array of selected shelter airports $j \in J$ for affected aircraft $i \in I$, which can be translated into the best-selected shelter airports for each affected aircraft with the nearest distance and shortest flight time from their current position.

3. Case study

This section presents a case study of a volcanic eruption, applying the mentioned approaches to a real situation of Mt.Hakone in Kanto peninsula, Kanagawa, Japan. One of Japan's most active volcanoes (JMA, 2019a) located in the middle of the busiest airspace and near air transportation hubs of Japan (i.e., Haneda and Narita airport international airport). The historical data observation from many sources included volcanic ash cloud pattern, and flight dataset (CARATS) was used to determine the affected area, airport, and aircraft from Mt.Hakone eruption. The data present in this section will be used in the proposed model validation (Section 4) and computational results (Section 5).

3.1. The affected airports

From the ashfall observation on Mt.Sakurajima located in South of Japan during the year 2009 to 2015 had discovered the pattern of ashfall during the period of eruption, typical plume height of explosion was between 2 and 5 km with the traceable of ashfall at least 70 km up to hundreds of kilometer away from the vent (JMA, 2019b). The ashfall direction and distribution were highly non-uniform, influenced by seasonal winds (Poulidis et al., 2018). During the selected period of the study in March, according to the latest CARATS flight dataset of March 2016 provided by Japan MLIT, wind's direction in the Kanto peninsula moves toward the East across this area. However, the wind profile's possible direction can be varied toward North-east and South-east to Pacific ocean with vary windspeed during day-time and night-time from 9.3 km/h. to 30 km/h. (JMA, 2019c). Based on these observations, the affected area was simulated by using geocoordinate (Latitude and Longitude) with the start point at Mt.Hakone volcano (35°14′00″N, 139°01′15″E) with varied direction toward North-east and South-east to the Pacific Ocean from 45°NE to 45°SE as shown in Fig. 5b.

The number of affected airports has increased related to the volcanic ash cloud's direction and coverage area/airspace. The simulated affected area and the CARATS dataset were used to determine the affected airports and the affected aircraft in the following sections. There were 5 airports within the simulated direction of ashfall; 3 of them were in the minimum range of ashfall, i.e., Oshima, Chofu, and Haneda (Tokyo) airport and others 2 airports within 200 km range from the vent. They could get impact from ashfall after the eruption within 2-7hrs and 5-16hrs, respectively. The 2 out of 5 airports are also Japan's major domestic and international airports: Haneda and Narita international airport, as shown in Fig. 5.

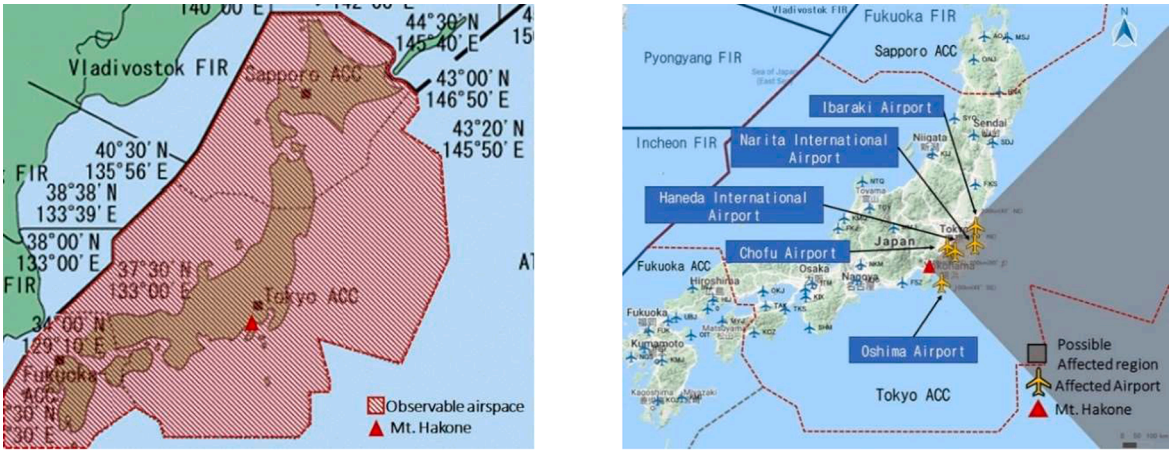

Fig. 5. Observable airspace according to CARATS flight dataset (a) and Map of possible affected area and airports (b), Japan Civil Aviation Bureau (JCAB), Ministry of Land, Infrastructure, Transport and Tourism (MLIT).

3.2. The affected aircrafts

Airborne aircraft: this study assumed that, at the moment of volcanic eruption, all pending departure aircraft with their itineraries to the affected airports would reroute their flight's itineraries to other safe airports to avoid the impact from a volcanic eruption. Therefore, the study was considered only airborne aircrafts with their possible inbound to the affected airports. From the latest CARATS flight data on March 2016 observation, the week's busiest day was on Sunday between 10:00 am – 9:00 pm. There were 7383 airborne aircrafts in the Japan airspace, with an average of 671 flights per hour. Among those flights, 15.8% or 107 aircrafts were inbound flights to the affected airports, which needed to be rerouted to safe shelter airports, and others were outbound or safe itinerary aircrafts. See Table 2.

On-ground aircraft: In this study, the maximum occupancy rate (*OCj*) were used to determine the number of affected aircraft and the affected airports. Those data were obtained from the flight schedule on June 2020 during the busiest period from 10:00 am to 9:00 pm of each affected airport; RJTO, RJTF, RJTT, RJAA, and RJAH at ~11%, 17%, 20%, 38%, and 20%, respectively (Central-Air, 2020; HND, 2020; IBR, 2020; NRT, 2020). Therefore, the number of affected on-ground aircraft at 5 airports was 154 aircrafts from their overall capacities at 535. The total number of observable affected aircraft from both airborne and on-ground were 261 aircrafts, Table 3.

Table 2
Aircraft size classification ratio by wingspan of 7,383 observable aircrafts in Japan airspace and 107 inbound airborne aircrafts to the affected airspace and airports.

Size Categories	7383 Observable airborne aircrafts: CARATS dataset[1]			Airborne Aircrafts[2]		
	ICAO Size Code_Letter	Number of aircraft	% of Total aircraft	ICAO Size Code_Letter	Number of aircraft	% of Total aircraft
Small	B	281	3.80%	B	2	1.90%
Medium	C	4,134	56.00%	C	58	54.70%
	D	783	10.60%	D	14	14.20%
Large	E	2,082	28.20%	E	32	29.20%
	F	103	1.40%	F	0	0.00%
	Total	**7,383**	**100.00%**	**Total**	**107**	**100.00%**

[1] Total flight from the CARATS flight data on March 2016, the busiest day of the week, Sunday between 10:00 am and 9:00 pm.
[2] calculated from an average 671 flights per hour, 15.8% was an inbound flight to 5 affected airports from 7383 observed aircraft on Sunday during 10:00 am–9:00 pm (the busiest day and time).

Table 3
Maximum number of observed affected aircraft using in the study provided by AIS and CARATS.

Observed Location	Airport	ICAO Code	Maximum aircraft stands[3]	Max_Occupancy per hour[4]	Affected aircraft (Occupied stands)	Affected aircraft by Aircraft's size[5]			Total
						Large	Medium	Small	
						29%	69%	2%	
On-ground: at affected airports (AIS)	Oshima	RJTO	9	11%	1	0	1	0	**154**
	Chofu	RJTF	24	17%	4	1	3	0	
	Tokyo	RJTT	228	20%	46	13	32	1	
	Narita	RJAA	266	38%	101	29	70	2	
	Ibaraki	RJAH	8	20%	2	1	1	0	
Airborne (CARATS),	Inbound to Affected airports		–			31	74	2	**107**
Grand Total									**261**

[3] Civil Aircraft: private and commercial aircraft.
[4] Refer to Appendix A Table A2.
[5] According to aircraft size ratio from observed historical flight data CARATS 7383 aircrafts.

3.3. The sheltering airports

This study has focused on shelter airport selection using the assumptions mention in Section 2.3.1 to ensure aircraft handling capabilities of the selected shelter airports during the evacuation and recovering in particularly suitability for the sizes of affected aircrafts. From the observation on 107 airborne aircrafts with an inbound itinerary to the affected airports, we had discovered that 54.7% of aircraft were in group C with the wingspan of 24 m up to (but less than) 36 m, which needed more than 1200 m up to (but less than) 1800 m of field length—followed by group E (29.2%), and D (14.2%), which need longer runway up to 3200 m. The ratio by wingspan of 107 airborne aircraft also identical to the 7383 observed aircrafts in the Japan airspace in the same time frame as shown in Table 2.

Overall, 98.13% of 107 inbound airborne aircrafts needed a field length of 1200 m and up to more than 3000 m to perform landing and taking off. We could assume that 154 on-ground aircrafts at the affected airports were at the same ratio as shown in Table 3. According to Japan's airports information provided by AIS, 82 from 94 airports or 88.3% of all Japan's airports could accommodate aircraft with code letter from C - F (medium - the larger-size of aircraft). The study is also considered airport connectivity, the capability of transferring affected crews and passengers to nearby accommodation facilities or nearby airports. Airport connectivity aims to allow affected crews and passengers be able to reach their final destinations. This study has chosen 42 airports on the mainland of Japan out of 94 airports outside the ash cloud affected area as the shelter airport candidates to maintain changing mode of transportation and connectivity capability (Smith and Arnedos, 2007), with an available capacity of up to 925 aircraft stands (all sizes), see Table A4. The available capacity used assumption of the average of maximum cumulative occupancy aircraft stands (OC_j) between the arrival and departure aircraft at 5 affected to determine number of the available aircraft stands at the 42 airports. The result shows that 21% of aircraft stands were occupied on average per hour during the busiest period, which could be assumed that 79% of airport capacity is non-occupancy or available aircraft stands rate (NC_j). See details in Table A2.

4. Models validation

The sensitivity analysis is the process to validate the behavior and outcome of the proposed models on GA and GRASP in this study using various values of specific parameter configurations used in the models. The validation and sensitivity analysis used the same dataset of the selected case study of Mt.Hakoke Japan in Section 3, with 261 affected aircrafts, 42 shelter airport candidates (5 affected airports excluded). The goal was to ensure that the proposed models could perform and give valid results according to the study's objective, subjective, and constraints on the various inputs.

The results have shown that both algorithms could perform and gave valid results as they had been designed in the proposed model. The details on the sensitivity analysis have been given in the followings:

4.1. Genetic algorithm: model validation and sensitivity analysis

In the genetic algorithm sensitivity analysis, the various values of specific parameter configurations: 1) crossover probability (CRXPB) and mutation probability (MUTPB), and 2) the ratio of affected aircraft, is investigated on the aircraft assigning pattern and outcomes. The suitable parameters which give the best result are used as the base-parameters configuration in this study to ensure it could perform and give a valid result.

Table 4
Parameters setting for the proposed model on genetic algorithm validation.

Parameter	Minimum value	Maximum value	(+) Incremental or (−) Decremental
Initial population	–	500	–
Crossover probability	0.00	1.00	+0.05
Mutation probability	0.00	1.00	+0.05
Number of iterations	–	500	–

Crossover and mutation probability parameters sensibility analysis: the various crossover and mutation probability parameters were used as shown in Table 4. The study had revealed that increasing crossover probability number from 0.0 to 1.0 had decreased the fitness value (minimum total flight time) and the number of the exceeded-capacity airport. Thus, increasing mutation probability from 0.0 to 1.0 had risen the fitness value of each generation caused by increased genes variation of the best-selected populations' offspring until all the genes within its chromosome were utterly different from its parents at the probability of 1.0. As a result, the algorithm assigned aircraft to fewer shelter airports until it had violated the airport capacity's constraint, which triggered penalty function to give the additional flight time to those solutions to get rid of them on the evaluation process. Consequently, higher mutation probability had given high fitness value: high total flight time and a higher number of exceeded-capacity airports that could not be used for aircraft evacuation, as shown in Fig. 6(b).

From the observation on crossover and mutation probabilities effect on GA outcome's behaviors, the acceptable range of the crossover and mutation probability numbers give low in total flight time, and a number of the capacity-exceeded airport could be varied between 0.50–1.00 and 0.10–0.60 respectively. According to the study's objective and subjective, the best crossover and mutation probability configuration was at 1.0 and 0.45, respectively, which gave the best fitness value of the lowest total flight time and not exceeding airport capacity. These probabilities were later used as the base configuration for GA. See Fig. 6(a) and Fig. 7(a) and (b).

Airport's occupancy rate sensitivity analysis: The varied airport occupancy rate was set to simulate the air traffic congestion level, reflecting on the airport's aircraft occupancy and availability rate. The airport's occupancy rate (OC_j) was set within the range of −20% to +20% of the baseline rate with an incremental and decremental rate of ±5%. See details in Table A3 and A4. Consequentially, increasing the shelter airport occupancy rate had increased the number of affected aircraft, which decreased the available aircraft stands for evacuation. It also indicated increasing air traffic congestion level and vice versa.

The sensitivity study has shown increasing occupancy rate (OC_j) by +20% of the baseline from 21% to 25.2%, decreasing the total number of non-occupancy rate (NC_j) of 42 shelter airports 925 to 856 stands or from 79% to 75%. The increasing OC_j rate also increased the congestion level in airspace and airport, which raised the total number of affected aircraft from 261 to 312 aircrafts, as shown in Table A3. Decreasing the non-occupancy stands at each shelter airport candidates forced the system to select further and more airports from 27 airports at baseline to 40 airports to accommodate the increased number of affected aircraft, as shown in Fig. 8 (b). As reflected on the objective function's value, the total flight time has increased from baseline at 104.75–168.16 h, see Fig. 8(a).

In contrast, decreasing the occupancy rate by −20% had increased the total number of the non-occupancy stand from 925 to 972 stands or 79–83%, respectively, which decreased the number of affected aircraft to 208 from baseline. The objective function value also dropped from baseline to 73.07 h. An increasing number of available stands at each shelter airport candidate close to the affected aircraft positions reduced the number of selected shelter airports from 27 to 21 airports. From the study, the proposed model applied to GA was able to perform and gave valid results in assigning aircraft to the nearest airports without exceeding their capacities by aircraft size through both baseline dataset and the various rate of occupied stand settings, as shown in Fig. 8.

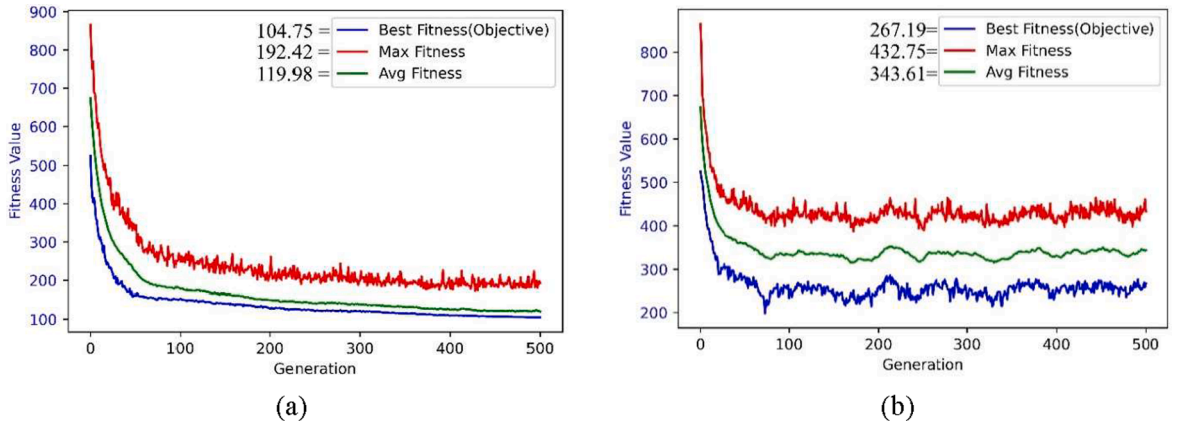

Fig. 6. GA performance at CRXPB 1.0 and MUTPB 0.45, 500 iterations: best result (a), and the highest result of the MUTPB at 1.0 (b).

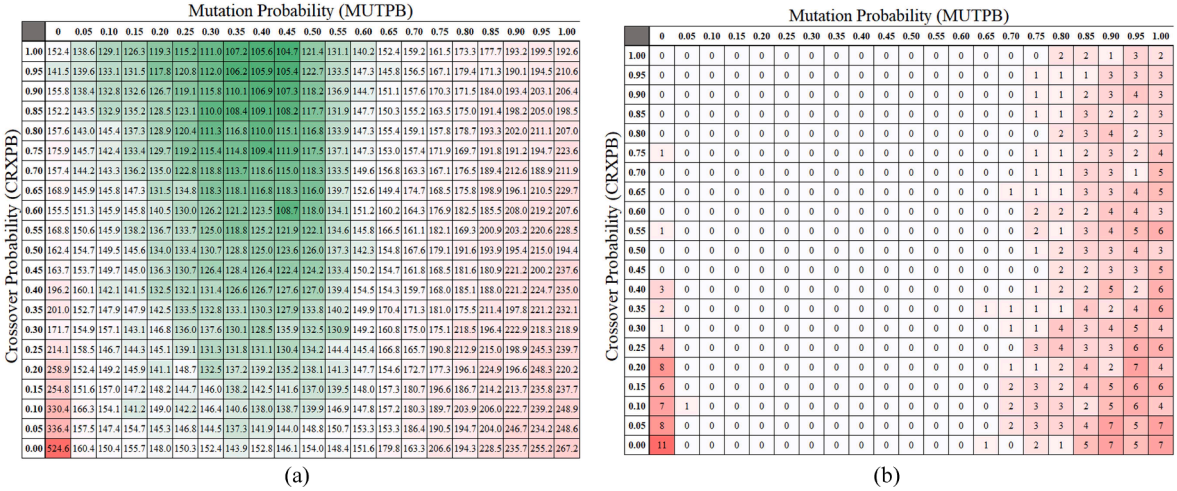

Fig. 7. Results of sensitivity analysis on various crossover and mutation probabilities: total flight time (a) and the number of the exceeded-capacity airport (b). The best result at minimum total flight time was 104.75hr, and the number of the exceeded-capacity airport was 0 at crossover and mutation probability 1.0 and 0.45, respectively.

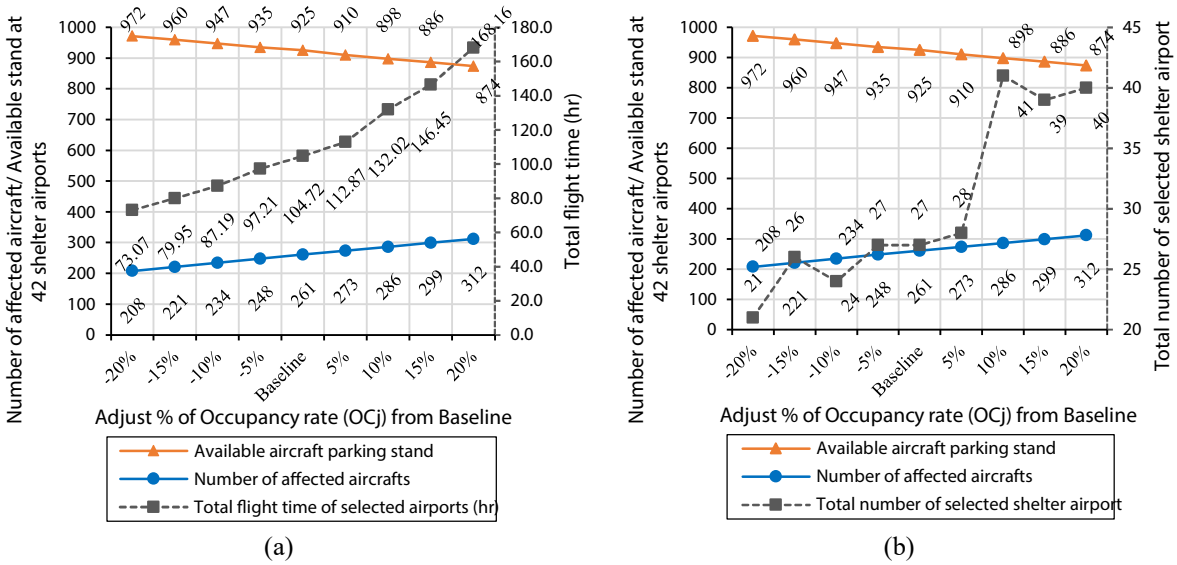

Fig. 8. The GA's results on a various simulated number of affected aircraft between −20% to +20% of baseline with decrement/increment rate at ±5%: (a) total flight time and (b) number of selected shelter airports.

4.2. GRASP: Model validation and sensitivity analysis

The first goal was the outcome validation, whether it could give the results according to the proposed model. According to the study dataset, the study's objective and subjective through baseline setting; the number of affected aircrafts, and available aircraft stands. The second goal was to investigate the model's behavior and outcome through the various value of inputs and the various ratio of the occupied stand settings used in GA; see detail in Table A3.

From the study, the proposed model was able to perform and gave valid results according to objective and subjective of the research in assigning aircraft to the nearest airports without exceeding their capacities by aircraft size on both baseline dataset and the various rate of the occupied aircraft stand. The result had shown the best solutions were selected through the process of randomly creating an initial solution, evaluating the solution against the subjective and constraints, comparing with the previous iteration's best solution before selection, and recording the better solution over 500 running iterations as it had been designed with decreased in the minimum number of total flight time and no exceeded-capacity airport as shows in Fig. 9(a) and (b)

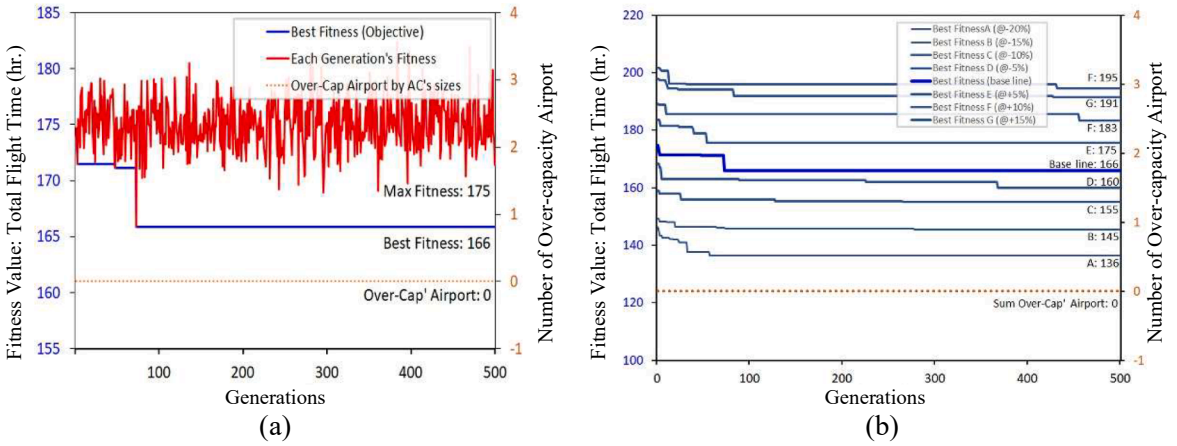

Fig. 9. GRASP's result for baseline affected aircraft (a), and the results of a various simulated number of affected aircraft between −20% to +20% of baseline with decrement/increment rate at ±5% (b).

5. Computational results

In this section, the proposed models applied on Genetic Algorithm (GA) and Greedy Randomized Adaptive Search Procedure (GRASP) were analyzed and compared their performances according to the study's objective and subjective mentioned in Section 2.3.1, included minimum in total flight time and shelter airport's capacity constraint by aircraft stands and affected aircrafts' sizes. The details of each algorithms' results and comparison have been presented as followed:

5.1. The genetic algorithms

In GAs, the affected aircrafts had been assigned to the nearest available shelter airport, similar to GRASP. Unlike the GRASP random mechanism, GA had a different mechanism through crossover and mutation called "the evolution mechanism". From the beginning of the process, 500 solutions of chromosomes were randomly generated, then evaluated their fitness against objective (1) and subjective (2)(3) along with penalty function in equation (4) to keep the model's solution from violating those subjective. Before selecting parents for the next generation, the reproduction through gene crossover and mutation to produce new alternative offspring could preserve and the alternate possibility of a solution before going through the fitness test's evaluation as the best solution for the objective's problem.

As a result, 27 out of 42 shelter airports have been selected for accommodating the aircrafts with a total flight time for evacuation of 104.75 h from 500 running iterations (duration 4.16 min), as shown in Table 5. Therefore, the time for each aircraft's evacuation was between 0.18 and 0.84 h, with an average of 0.44 h. The aircraft distribution was between 0.4% and 22.6%, with 3.7% on average of the total number of affected aircrafts. The maximum capacity usage at the selected shelter airports had been utilized between 5.9 and 92.2%, with the average at 42.3% of their available stands (non-occupancy stands). According to the airport's capacity based on the aircraft sizes constraint within penalty function, there was no exceeded the number of affected aircraft assigned to any selected shelter airport. The model also addressed the first 5 critical airports on the scenario, which accommodates 61.7% of the affected aircraft population. They were Chūbu centrair international airport (RJGG) 22.6%, Kansai international airport (RJBB) 14.9%, Osaka international airport (RJOO) 14.6%, Niigata airport (RJSN) 4.98%, and Sendai airport (RJSS) 4.60%, as shown in Fig. 10(a) and Table A1.

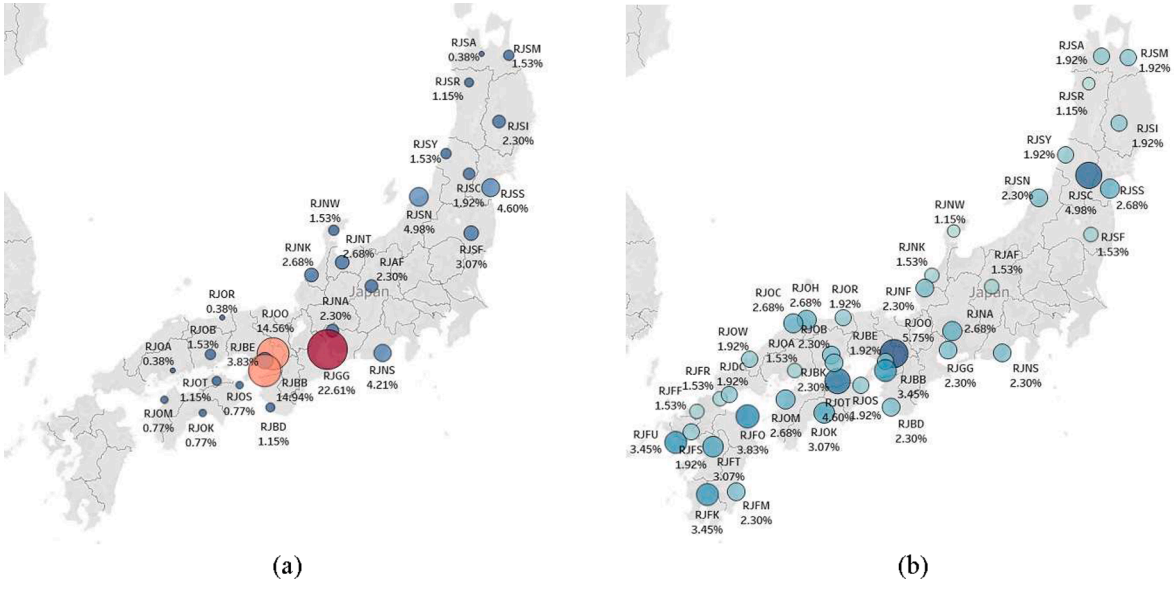

Fig. 10. Mapping of assigned aircrafts to shelter airport by using Genetic algorithms (a), Mapping of aircrafts distribution to shelter airport by using GRASP (b).

Table A1
Aircraft Stands Utilization result from GA and GRASP: by Affected Aircraft and Aircraft Stand Sizes.

Airport Name	ICAO Code	IATA Code	Airport Capacity by Sizes (Aircraft Stands)								Computational Results													
			Maximum Capacity				Available capacity: Assumption of non-occupancy stand rate = 79% of Max Capacity (Table A2)				Aircraft Stands Utilization by Aircraft and Stand Sizes: Genetic Algorithm (GA)							Greedy Randomized Adaptive Search Procedure (GRASP)						
			Small	Medium	Large	Total Capacity	Small	Medium	Large	Total Capacity	Rank	Small	Medium	Large	Total	Overvall Capacity usage per available cap	% of All Affected Aircrafts	Rank	Small	Medium	Large	Total	Overvall Capacity usage per available cap	% of All Affected Aircrafts
Chūbu Centrair International Airport	RJGG	NGO	6	30	44	80	5	24	35	64	1	0	24	35	59	92.19%	22.61%	4	0	10	2	12	18.75%	4.60%
Kansai International Airport	RJBB	KIX	12	45	10	67	9	36	8	53	2	0	31	8	39	73.58%	14.94%	3	0	11	2	13	24.53%	4.98%
Osaka International Airport	RJOO	ITM	0	33	27	60	0	26	21	47	3	0	26	12	38	80.85%	14.56%	5	0	11	1	12	25.53%	4.60%
Niigata Airport	RJSN	KIJ	14	10	5	29	11	8	4	23	4	1	8	4	13	56.52%	4.98%	8	0	7	2	9	39.13%	3.45%
Sendai Airport	RJSS	SDJ	33	10	4	47	26	8	3	37	5	1	8	3	12	32.43%	4.60%	6	0	8	3	11	29.73%	4.21%
Shizuoka Airport	RJNS	FSZ	6	7	4	17	5	6	3	14	6	2	6	3	11	78.57%	4.21%	7	1	6	3	10	71.43%	3.83%
Kobe Airport	RJBE	UKB	0	10	4	14	0	8	3	11	7	0	7	3	10	90.91%	3.83%	11	0	4	3	7	63.64%	2.68%
Fukushima Airport	RJSF	FKS	10	5	3	18	8	4	2	14	8	2	4	2	8	57.14%	3.07%	16	0	4	2	6	42.86%	2.30%
Komatsu Airport	RJNK	KMQ	2	6	3	11	2	5	2	9	9	0	5	2	7	77.78%	2.68%	12	0	5	2	7	77.78%	2.68%
Toyama Airport	RJNT	TOY	12	6	1	19	9	5	1	15	10	1	5	1	7	46.67%	2.68%	17	0	5	1	6	40.00%	2.30%
Nagoya Airport	RJNA	NKM	73	5	2	80	58	4	2	64	11	0	4	2	6	9.38%	2.30%	18	0	4	2	6	9.38%	2.30%
Hanamaki Airport	RJSI	HNA	19	5	2	26	15	4	2	21	12	0	4	2	6	28.57%	2.30%	22	0	4	1	5	23.81%	1.92%
Matsumoto Airport	RJAF	MMJ	11	3	1	15	9	2	1	12	13	3	2	1	6	50.00%	2.30%	13	4	2	1	7	58.33%	2.68%
Yamagata Airport	RJSC	GAJ	6	5	1	12	5	4	1	10	14	1	3	1	5	50.00%	1.92%	23	0	4	1	5	50.00%	1.92%
Misawa Airport	RJSM	MSJ	21	3	2	26	17	2	2	21	15	1	1	2	4	19.05%	1.53%	28	0	2	2	4	19.05%	1.53%
Noto Airport	RJNW	NTQ	4	3	1	8	3	2	1	6	16	1	2	1	4	66.67%	1.53%	33	0	2	1	3	50.00%	1.15%
Okayama Airport	RJOB	OKJ	6	5	2	13	5	4	2	11	17	0	2	2	4	36.36%	1.53%	38	0	1	1	2	18.18%	0.77%
Shonai Airport	RJSY	SYO	7	4	1	12	6	3	1	10	18	0	3	1	4	40.00%	1.53%	29	0	3	1	4	40.00%	1.53%
Takamatsu Airport	RJOT	TAK	18	7	3	28	14	6	2	22	19	0	1	2	3	13.64%	1.15%	24	0	4	1	5	22.73%	1.92%
Nanki-Shirahama Airport	RJBD	SHM	6	3	1	10	5	2	1	8	20	0	2	1	3	37.50%	1.15%	34	0	2	1	3	37.50%	1.15%
Odate-Noshiro Airport	RJSR	ONJ	4	4	1	9	3	3	1	7	21	0	2	1	3	42.86%	1.15%	30	0	3	1	4	57.14%	1.53%
Tokushima Airport	RJOS	TKS	10	4	2	16	8	3	2	13	22	0	1	1	2	15.38%	0.77%	25	0	3	2	5	38.46%	1.92%
Kōchi Airport	RJOK	KCZ	12	6	3	21	9	5	2	16	23	0	0	2	2	12.50%	0.77%	14	0	5	2	7	43.75%	2.68%
Matsuyama Airport	RJOM	MYJ	16	7	4	27	13	6	3	22	24	0	1	1	2	9.09%	0.77%	35	0	2	1	3	13.64%	1.15%
Hiroshima Airport	RJOA	HIJ	3	6	3	12	2	5	2	9	25	0	1	0	1	11.11%	0.38%	39	0	2	0	2	22.22%	0.77%
Aomori Airport	RJSA	AOJ	13	3	3	19	10	2	2	14	26	0	1	0	1	7.14%	0.38%	31	0	2	2	4	28.57%	1.53%
Tottori Airport	RJOR	TTJ	18	3	1	22	14	2	1	17	27	0	1	0	1	5.88%	0.38%	36	0	2	1	3	17.65%	1.15%
Kōnan Airport	RJBK	0	61	3	0	64	48	2	0	50	28	0	0	0	0	0.00%	0.00%	40	0	2	0	2	4.00%	0.77%
Miho-Yonago Airport	RJOH	YGJ	10	5	2	17	8	4	2	14	29	0	0	0	0	0.00%	0.00%	37	0	3	0	3	21.43%	1.15%
Fukuoka Airport	RJFF	FUK	36	40	20	96	28	32	16	76	30	0	0	0	0	0.00%	0.00%	19	1	4	1	6	7.89%	2.30%
Kagoshima Airport	RJFK	KOJ	23	9	3	35	18	7	2	27	31	0	0	0	0	0.00%	0.00%	9	0	7	2	9	33.33%	3.45%
Kitakyūshū Airport	RJFR	KKJ	18	9	3	30	14	7	2	23	32	0	0	0	0	0.00%	0.00%	20	0	5	1	6	26.09%	2.30%
Kumamoto Airport	RJFT	KMJ	28	6	2	36	22	5	2	29	33	0	0	0	0	0.00%	0.00%	15	0	5	2	7	24.14%	2.68%
Miyazaki Airport	RJFM	KMI	3	16	6	25	2	13	5	20	34	0	0	0	0	0.00%	0.00%	10	1	4	3	8	40.00%	3.07%
Nagasaki Airport	RJFU	NGS	8	7	3	18	6	6	2	14	35	0	0	0	0	0.00%	0.00%	2	6	6	2	14	100.00%	5.36%
Oita Airport	RJFO	OIT	3	5	3	11	2	4	2	8	36	0	0	0	0	0.00%	0.00%	26	0	4	1	5	62.50%	1.92%
Yamaguchi Ube Airport	RJDC	UBJ	8	6	3	17	6	5	2	13	37	0	0	0	0	0.00%	0.00%	21	0	4	2	6	46.15%	2.30%
New Chitose Airport	RJCC	CTS	10	45	15	70	8	36	12	56	38	0	0	0	0	0.00%	0.00%	1	0	17	2	19	33.93%	7.28%
Fukui Airport	RJNF	FKJ	1	0	0	1	1	0	0	1	39	0	0	0	0	0.00%	0.00%	42	0	0	0	0	0.00%	0.00%
Iwami Airport	RJOW	IWJ	0	3	0	3	0	2	0	2	40	0	0	0	0	0.00%	0.00%	41	0	2	0	2	100.00%	0.77%
Izumo Airport	RJOC	IZO	5	5	1	11	4	4	1	9	41	0	0	0	0	0.00%	0.00%	32	0	4	0	4	44.44%	1.53%
Saga Airport	RJFS	HSG	10	5	1	16	8	4	1	13	42	0	0	0	0	0.00%	0.00%	27	0	4	1	5	38.46%	1.92%
Total			***566***	***402***	***200***	***1168***	***446***	***320***	***159***	***925***		***13***	***155***	***93***	***261***		***100%***		***13***	***189***	***59***	***261***		***100%***

5.2. The Greedy Randomized Adaptive Search Procedure (GRASP)

In GRASP, the affected aircrafts had been assigned to the nearest shelter airport available by using the distance from the current position of each affected aircrafts. Moreover, the airport's capacity by aircraft size was considered to prevent the algorithm from assigning aircraft to the selected airport, as shown in Table A1. GRASP has the mechanism of searching, evaluating, selecting the best solution, and generating a new solution through the random number process. It can search and replace the better solution from the given conditions and constraints. From 500 running iterations, 2.21 min were used to search for the best solution against total flight time and shelter airport capacities by aircraft size constraints with the best solution of 166.32 h in Table 5.

The results on shelter airport selection and aircraft distribution had shown that 41 shelter airports had been selected for accommodating affected aircrafts with a small distribution rate between 1.0% and 7.3% of the total number of affected aircrafts with no exceeded capacity at selected shelter airports. The algorithm had also addressed the first 5 critical airports, which accommodate 26.8% of the affected aircraft population. There were New Chitose airport (RJCC) 7.28%, Nagasaki airport (RJFU) 5.36%, Kansai international airport (RJBB) 4.98%, Chubu centrair international airport (RJGG), and Osaka international airport (RJOO) at 4.6%, as shown in see Fig. 10(b), and more details in Table A1.

5.3. Algorithm's performances comparison

From the performance results of the proposed models applied on Genetic Algorithm (GA) and Greedy Randomized Adaptive Search Procedure (GRASP), the study has shown the same algorithm iterations of 500 with the same set of total affected aircraft number, shelter airports, and capacity constraint by aircraft's sizes according to the study and algorithms' objective and subjective. The proposed model using GA could generate the better solution for aircrafts assignment to shelter airports with 104.75 h of total flight time (TFT) or −63.0% compared to 166.32 h from GRASP. Both algorithms can search for the solution with no over-capacity at the selected shelter airport even though GRASP searching duration was twice faster than in GA at 2.21 min to 4.16 min. Moreover, the study had tried to the extended iteration of GRASP to a critical of 200,000 iterations. At this critical iteration, the best result that GRASP could give was 161.34 h or 2.99% better than the result at 500 iterations. Thus, GRASP could not find a better solution than the proposed model on GA at the same running iterations or on the extended one in this study. The GRASP and GA performance comparison is shown below.

Table 5
Performance comparison between GA and GRASP.

Performance Criteria	GA	GRASP	Differentiation Rate (GA/GRASP)
Running Iterations	500		–
number of Aircraft	261		–
Number of Candidate shelter airports	42		–
Available aircraft aircrafts	925		–
Actual Total Flight Time by Distance	104.75	166.32	−63.0%
Number of Selected Airport	27	41	−66.0%
Number of Exceed-capacity Airport	0	0	–
Searching Duration (min)	4.16	2.21	+188.2%
μ: mean of flight Time(h)	0.44	0.64	−68.80%
Minimum flight Time(h)	0.18	0.06	+300.00%
Maximum flight Time(h)	0.84	1.29	−65.10%
Median	0.41	0.62	−66.10%
σ: STD	0.12	0.31	−38.70%
50th Percentile	0.41	0.62	−66.10%
80th Percentile	0.56	0.97	−57.70%
90th Percentile	0.56	1.14	−49.10%

6. Conclusion

This study has proposed the conceptual models for shelter airport selection for aircraft evacuation in a volcanic eruption by considering evacuation flight time and maximum shelter airport capacity. The models have been tested with a case study of a volcanic eruption at Mt. Hakone in Japan's central and the latest air traffic data in March 2016 (CARATS open dataset) provided by MLIT. The airport facilities data by AIS, and airlines flight schedules at each airport are also used to determine the number of the affected area, airports, the number of affected aircrafts and the available aircraft stands for evacuation during the event. The 261 affected aircrafts of both airborne and on-ground have been simulated their current positions and select the appropriate shelter airports for evacuation. For this study, 42 out of 94 airports had been chosen as shelter airports by criteria of location on the mainland of Japan for maintaining connectivity with other modes of transportations, outside ash cloud affected area, and sufficient runway's length for accommodating affected aircraft with 925 available aircraft stands (non-occupancy stands).

The proposed models had been applied to the Genetic Algorithm (GA) and Greedy Randomized Adaptive Search Procedure (GRASP) to find the approximate solution of shelter airport selection. Both algorithms proved their capabilities of searching for the approximate solution according to the study objective and subjective of the assigned aircraft to shelter airport with minimum total flight time, and not exceeding selected airports' capacities. With the same logical model of aircrafts assignment and running iteration, GA had outperformed GRASP to find less in total flight time solution for the overall population with fewer selected shelter airports on the case study. Since they were different in the best solution selection mechanism as mentioned in the computational results section, this gave GA's mechanism the advantage in preserving and passing on the previous best solution to its offspring through crossover operation.

Nevertheless, the study had also revealed the critical shelter airports for aircrafts evacuation. The larger-size airport with a large number of available aircraft stands is likely to act as the critical shelter airport during the disaster event, as shown in Appendix A-Table A1. The alternative adjustment of the proportion of available aircraft stands at shelter airports, along with the proportion of affected aircrafts, will give flexibility to the algorithms' output, which gives the better suggestion on which shelter airports could accommodate a reasonable number of aircraft according to their capacities.

The study could act as a suggestion for the authorities for the airport and aircraft emergency evacuation planning. However, this study could give a conceptual model of shelter airport selection solution for aircrafts evacuation in the volcanic eruption event using the nearest distances and airport capacity by aircraft size constraints. It still has limitations depending on the regulation's complexity at the airport, airline, and air traffic management, as mentioned earlier. The further applications on airport selection may need to set up more objectives and constraints for the shelter airport selection algorithm to effectively provide a more realistic selection from the beginning of evacuation until recovering for all sections of aircraft, passengers, and cargo and flight crew scheduling.

7. Limitations

This study's main limitations were subject to the unavailable data as follows: the accurate number of affected aircraft and their itineraries data for both airborne and on-ground, historical data of volcanic ash cloud coverage area, and its range from Mt.Hakone.

Although the number of affected aircraft were observed from the historical data before the pandemic, the aircraft stand occupancy rate and available of aircraft stands at candidate shelter airports in this study may not represent the normal air traffic situation of this region during the COVID-19 pandemic, which caused declined in most airline and airport operations by 90% (ICAO, 2020). Hence, the historical flight schedule data of shelter airports before the pandemic are required for the occupancy rate calculation accuracy to reflect the air traffic level's normal situation. However, this study's proposed model has allowed the occupancy rate adjustment to reflecting air traffic congestion level close to the level before the pandemic.

Furthermore, the unavailable ash cloud historical data of Mt.Hakone, the Sakurajima's volcanic ashfall, and ash cloud were studied to understand the ash cloud's behavior, which was used to predict and determine the possible ash cloud coverage area in the case study.

CRediT authorship contribution statement

Saharat Arreeras: Conceptualization, Investigation, Writing - original draft, Writing - review & editing. **Mikiharu Arimura:** Conceptualization, Funding acquisition, Project administration, Resources, Supervision.

Declaration of Competing Interest

The authors declare that they have no known competing financial interests or personal relationships that could have appeared to influence the work reported in this paper.

Acknowledgements

The authors wish to acknowledge the Ministry of Land, Infrastructure and Tourism (Japan) for supporting CARATS open dataset, as well as the study group of Kyoto University Disaster Prevention Research Institute "Study on Crisis Management System for Air Transport during Large-Scale Eruption".

Appendix A

Table A2
Arrival and departure flight per hour at 5 affected airports, aircraft stand occupancy rate, and an assumption of shelter airport available capacities.

Hour_Periods		Number of Flight per hour																				Average Cumulative Flight
		Oshima Airport				Chofu Airport				Narita International Airport				Ibaraki Airport				Haneda International Airport				
Start	End	Arrival	Departure	**Cumulative**	Total	Arrival	Departure	**Cumulative**	Total	Arrival	Departure	**Cumulative**	Total	Arrival	Departure	**Cumulative**	Total	Arrival	Departure	**Cumulative**	Total	
	12:00:00 AM	12:59:00 AM	0	0	**1**	0	0	0	**4**	0	0	0	**2**	0	0	0	**2**	0	0	0	**132**	0	28
	1:00:00 AM	1:59:00 AM	0	1	**0**	1	0	1	**3**	1	0	0	**2**	0	0	0	**2**	0	0	3	**129**	3	27
	2:00:00 AM	2:59:00 AM	0	0	**0**	0	0	0	**3**	0	0	0	**2**	0	0	0	**2**	0	2	0	**131**	2	28
	3:00:00 AM	3:59:00 AM	0	0	**0**	0	0	0	**3**	0	0	0	**2**	0	0	0	**2**	0	2	0	**133**	2	28
	4:00:00 AM	4:59:00 AM	0	0	**0**	0	0	0	**3**	0	0	0	**2**	0	0	0	**2**	0	3	0	**136**	3	29
	5:00:00 AM	5:59:00 AM	0	0	**0**	0	0	0	**3**	0	0	0	**2**	0	0	0	**2**	0	7	0	**143**	7	30
	6:00:00 AM	6:59:00 AM	0	0	**0**	0	0	0	**3**	0	8	0	**10**	8	0	0	**2**	0	7	37	**113**	44	26
	7:00:00 AM	7:59:00 AM	0	0	**0**	0	0	0	**3**	0	11	4	**17**	15	0	1	**1**	1	8	68	**53**	76	15
	8:00:00 AM	8:59:00 AM	0	0	**0**	0	0	0	**3**	0	14	4	**27**	18	0	1	**0**	1	45	51	**47**	96	15
	9:00:00 AM	9:59:00 AM	0	0	**0**	0	0	0	**3**	0	19	17	**29**	36	2	0	**2**	2	42	48	**41**	90	15
	10:00:00 AM	10:59:00 AM	0	0	**0**	0	0	2	**1**	2	12	23	**18**	35	2	1	**3**	3	45	40	**46**	85	14
	11:00:00 AM	11:59:00 AM	0	0	**0**	0	0	1	**0**	1	13	20	**11**	33	0	1	**2**	1	48	54	**40**	102	11
	12:00:00 PM	12:59:00 PM	0	0	**0**	0	3	0	**3**	3	10	13	**8**	23	1	0	**3**	1	35	55	**20**	90	7
	1:00:00 PM	1:59:00 PM	0	0	**0**	0	0	2	**1**	2	13	14	**7**	27	1	3	**1**	4	56	57	**19**	113	6
	2:00:00 PM	2:59:00 PM	0	0	**0**	0	0	0	**1**	0	19	12	**14**	31	0	0	**1**	0	41	45	**15**	86	6
	3:00:00 PM	3:59:00 PM	1	0	**1**	1	3	0	**4**	3	31	5	**40**	36	0	1	**0**	1	41	38	**18**	79	13
	4:00:00 PM	4:59:00 PM	0	0	**1**	0	0	0	**4**	0	24	12	**52**	36	0	0	**0**	0	37	34	**21**	71	16
	5:00:00 PM	5:59:00 PM	0	0	**1**	0	0	0	**4**	0	19	37	**34**	56	1	0	**1**	1	39	50	**10**	89	10
	6:00:00 PM	6:59:00 PM	0	0	**1**	0	0	0	**4**	0	12	25	**21**	37	0	1	**0**	1	45	45	**10**	90	7
	7:00:00 PM	7:59:00 PM	0	0	**1**	0	0	0	**4**	0	14	7	**28**	21	1	1	**0**	2	42	50	**2**	92	7
	8:00:00 PM	8:59:00 PM	0	0	**1**	0	0	0	**4**	0	7	9	**26**	16	2	0	**2**	2	53	28	**27**	81	12
	9:00:00 PM	9:59:00 PM	0	0	**1**	0	0	0	**4**	0	5	15	**16**	20	0	0	**2**	0	63	12	**78**	75	20
	10:00:00 PM	10:59:00 PM	0	0	**1**	0	0	0	**4**	0	1	11	**6**	12	0	0	**2**	0	37	4	**111**	41	25
	11:00:00 PM	11:59:00 PM	0	0	**1**	0	0	0	**4**	0	0	2	**4**	2	0	0	**2**	0	7	1	**117**	8	26
The busiest period																							
	Max_Capacity		9				24				266				8				228				% Avg_Occupency
	Min_Occupency	0	0	0	0	0	0	0	0	7	5	7	16	0	0	0	0	35	28	2	71	2	
	% Min_Occupency per cap	0%	0%	0%	0%	0%	0%	0%	0%	3%	2%	3%	6%	0%	0%	0%	0%	15%	12%	1%	31%	1%	
	Max_Occupency	**1**	**0**	**1**	**1**	**3**	**2**	**4**	**3**	**31**	**37**	**52**	**56**	**2**	**3**	**3**	**4**	**56**	**57**	**46**	**113**	**21**	
	****% Max_Occupency per cap**	**11%**	**0%**	**11%**	**11%**	**13%**	**8%**	**17%**	**13%**	**12%**	**14%**	**20%**	**21%**	**25%**	**38%**	**38%**	**50%**	**25%**	**25%**	**20%**	**50%**	**21%**	
	*****an assumption of 42 shelter airport available capacities, calculated from average(%Max_Occupency) of 5 affected airports: (1-0.21)**																					**79%**	

*Cumulative number between arrival and departure flight per hour can be assumed as aircraft stand occupancy per hour

**used as number of on-ground affected aircraft at 5 affected airports

*Cumulative number between arrival and departure flight per hour can be assumed as aircraft stand occupancy per hour.
**used as number of on-ground affected aircraft at 5 affected airports.

Table A3
Detail of affected aircraft, occupancy, and availability rate at the study airports with various simulated rate for the proposed models' configurations.

	Occupancy aircraft stand, Decrement/Increment rate at ±5%		Baseline *		-20%		-15%		-10%		-5%		5%		10%		15%		20%	
Airborne aircraft	Observable affected aircraft (CARATS dataset)	Number of affected aircraft	107		86		91		96		102		112		118		123		128	
On-ground aircraft at 5 affected airports	Affected Airports	Affected Airport Capacity	Max stand occupancy rate * (baseline)	Numbr of affected aircraft	Max stand occupancy rate (baseline -20%)	Number of affected aircraft (baseline -20%)	Max stand occupancy rate (baseline -15%)	Number of affected aircraft (baseline-15%)	Max stand occupancy rate (baseline -10%)	Number of affected aircraft (baseline -10%)	Max stand occupancy rate (baseline -5%)	Number of affected aircraft (baseline -5%)	Max stand occupancy rate (baseline +5%)	Number of affected aircraft (baseline +5%)	Max stand occupancy rate (baseline +10%)	Number of affected aircraft (baseline +10%)	Max stand occupancy rate (baseline +15%)	Number of affected aircraft (baseline +15%)	Max stand occupancy rate (baseline +20%)	Number of affected aircraft (baseline +20%)
	Oshima	9	11%	1	8.8%	1	9.4%	1	9.9%	1	10.5%	1	11.6%	1	12.1%	1	12.7%	1	13.2%	1
	Chofu	24	17%	4	13.6%	3	14.5%	3	15.3%	4	16.2%	4	17.9%	4	18.7%	4	19.6%	5	20.4%	5
	Tokyo (Haneda)	228	20%	46	16.0%	36	17.0%	39	18.0%	41	19.0%	43	21.0%	48	22.0%	50	23.0%	52	24.0%	55
	Narita	266	38%	101	30.4%	81	32.3%	86	34.2%	91	36.1%	96	39.9%	106	41.8%	111	43.7%	116	45.6%	121
	Ibaraki	8	20%	2	16.0%	1	17.0%	1	18.0%	1	19.0%	2	21.0%	2	22.0%	2	23.0%	2	24.0%	2
	Total number of affected aircraft			154		122		130		138		146		161		168		176		184
	Grand total of affected aircraft			**261**		**208**		**221**		**234**		**248**		**273**		**286**		**299**		**312**

Table A4
Detail of available aircraft stands (non-occupancy stands) at 42 shelter airports.

Occupancy aircraft stand, Decrement/Increment rate at ±5%	Baseline *	−20%	−15%	−10%	−5%	5%	10%	15%	20%
Overall capacity of 42 shelter airports	1168								
Average aircraft stand occupancy rate (c_j) **	21%	16.8%	17.9%	18.9%	20.0%	22.1%	23.1%	24.2%	25.2%
Average aircraft stand availability rate	79%	83%	82%	81%	80%	78%	77%	76%	75%
Average available capacity	**925**	**972**	**960**	**947**	**935**	**910**	**898**	**886**	**874**

* the maximum aircraft stand occupancy was calculated from the maximum cumulative number of aircraft stand occupancy at 5 affected airports, refer to Table A2.
** the average aircraft stand occupancy was calculated from average maximum number of aircraft stand occupancy at 5 affected airports at 21% of airport's capacity, refer to Table A2.

Table A5
Aerodrome Design and Operations, Aerodrome reference code in Annex 14 - volume 1: by ICAO.

Runway		Aero plane		
Code Name	Aero plane reference field length	Code Letter	Wingspan	Outer main gear wheel span
1	<800 m	A	<15 m	<4.5 m
2	800 m up to but not including 1200 m	B	15 m but < 24 m	4.5 m but < 6 m
3	1200 m up to but not including 1800 m	C	24 m but < 36 m	6 m but < 9 m
4	1800 m and over	D	36 m but < 52 m	9 m but < 14 m
		E	52 m but < 65 m	9 m but < 14 m
		F	65 m but < 80 m	14 m but < 16 m

References

Airbus, 2005. Airbus A320 Aircraft Characteristics, Airport and Maintenance Planning. Airbus S.A.S. 1–387.
Aktel, A., Yagmahan, B., Özcan, T., Yenisey, M.M., Sansarcı, E., 2017. The comparison of the metaheuristic algorithms performances on airport gate assignment problem. Transp. Res. Procedia 22, 469–478. https://doi.org/10.1016/j.trpro.2017.03.061.
Button, K., Vega, H., Nijkamp, P., 2010. A dictionary of transport analysis, a dictionary of transport analysis. Doi: 10.4337/9781849804714.
Central-Air, 2020. 新中央航空株式会社 Time Table [WWW Document]. URL https://www.central-air.co.jp/en/timetable.html (accessed 2.13.20).
Cheng, C.H., Ho, S.C., Kwan, C.L., 2012. The use of meta-heuristics for airport gate assignment. Expert Syst. Appl. 39, 12430–12437. https://doi.org/10.1016/j.eswa.2012.04.071.
Cidell, J., 2006. Regional cooperation and the regionalization of air travel in Central New England. J. Transp. Geogr. 14, 23–34. https://doi.org/10.1016/j.jtrangeo.2004.10.003.
Costea, O., 2011. Airbus A380 aircraft characteristics airport and maintenance planning AC.
De Rainville, F.-M., Fortin, F.-A., Gardner, M.-A., Parizeau, M., Gagné, C., 2012. DEAP. In: Proceedings of the Fourteenth International Conference on Genetic and Evolutionary Computation Conference Companion - GECCO Companion '12. ACM Press, New York, New York, USA, p. 85. Doi: 10.1145/2330784.2330799.
Dell'Orco, M., Marinelli, M., Altieri, M.G., 2017. Solving the gate assignment problem through the Fuzzy Bee Colony Optimization. Transp. Res. Part C Emerg. Technol. 80, 424–438. https://doi.org/10.1016/j.trc.2017.03.019.
Ding, H., Lim, A., Rodrigues, B., Zhu, Y., 2005. The over-constrained airport gate assignment problem. Comput. Oper. Res. 32, 1867–1880. https://doi.org/10.1016/j.cor.2003.12.003.
Feo, T.A., Resende, M.G.C., 1995. Greedy randomized adaptive search procedures. J. Glob. Optim. 6, 109–133. https://doi.org/10.1007/BF01096763.
Guépet, J., Acuna-Agost, R., Briant, O., Gayon, J.P., 2015. Exact and heuristic approaches to the airport stand allocation problem. Eur. J. Oper. Res. 246, 597–608. https://doi.org/10.1016/j.ejor.2015.04.040.
Hanaoka, S., Indo, Y., Hirata, T., Todoroki, T., Aratani, T., Osada, T., 2013. Lessons and challenges in airport operation during a disaster: case studies on Iwate Hanamaki airport, Yamagata airport, and Fukushima airport during the great east japan earthquake. J. JSCE 1, 286–297. https://doi.org/10.2208/journalofjsce.1.1_286.
Harriman, S., Fanjoy, R., Petrin, D., 2009. Small general aviation airport emergency preparedness and the perceived risks of very light jet operations. J. Aviat. Educ. Res. https://doi.org/10.15394/jaaer.2009.1382.
Harsha, P., 2003. Mitigating Airport Congestion: Market Mechanisms and Airline Response Models. Massachusetts Institute of Technology.
HND, 2020. Tokyo Haneda International Airport (HND/RJTT) | Arrivals, Departures & Routes | Flightradar24 [WWW Document]. accessed 2.13.20. https://www.flightradar24.com/data/airports/hnd.
Horner, M.W., Downs, J.A., 2010. Optimizing hurricane disaster relief goods distribution: model development and application with respect to planning strategies. Disasters. https://doi.org/10.1111/j.1467-7717.2010.01171.x.
Hu, F., Yang, S., Xu, W., 2014. A non-dominated sorting genetic algorithm for the location and districting planning of earthquake shelters. Int. J. Geogr. Inf. Sci. https://doi.org/10.1080/13658816.2014.894638.
Hu, Y., Song, Y., Zhao, K., Xu, B., 2016. Integrated recovery of aircraft and passengers after airline operation disruption based on a GRASP algorithm. Transp. Res. Part E Logist. Transp. Rev. 87, 97–112. https://doi.org/10.1016/j.tre.2016.01.002.
IBR, 2020. Flight information | Ibaraki Airport [WWW Document]. accessed 2.12.20. http://www.ibaraki-airport.net/en/flight.html.
ICAO, 2020. FEB 2020 : Air Transport Monthly Monitor FEB 2020 : Air Transport Monthly Monitor 2019–2020.
ICAO, 2019. ASSEMBLY-40TH SESSION EXECUTIVE COMMITTEE Agenda Item 26: Other high-level policy issues to be considered by the Executive Committee GET AIRPORT READY FOR DISASTER.
ICAO, 2016. Annex 14: Aerodrome Design and Operations Seventh Edition, International Civil Aviation Organization.
ICAO, 2013. ICAO Environmental Report 2013. ICAO Environ. Rep. 2013.
Jimenez Serrano, F.J., Kazda, A., 2017. Airline disruption management: Yesterday, today and tomorrow. In: Transportation Research Procedia. Elsevier, pp. 3–10. Doi: 10.1016/j.trpro.2017.12.162.
JMA, 2019a. Volcanic Warning [WWW Document]. Japan Meteorol. Angency. URL https://www.jma.go.jp/en/volcano/ (accessed 6.1.19).
JMA, 2019b. Sakurajima Continuously Monitored [WWW Document]. Janpan Meteorol. Agency. URL https://www.data.jma.go.jp/svd/vois/data/tokyo/STOCK/souran_eng/volcanoes/090_sakurajima.pdf (accessed 8.26.19).
JMA, 2019c. Climat of Kanto/Koshin district [WWW Document]. Janpan Meteorol. Agency. URL https://www.data.jma.go.jp/gmd/cpd/longfcst/en/tourist/file/Kanto_Koshin.html (accessed 9.15.19).

Kita, H., Koike, A., Tanimoto, K., 2005. Air service development of local airports and its influence on the formation of aviation networks. Res. Transp. Econ. https://doi.org/10.1016/S0739-8859(05)13011-X.
Kongsomsaksakul, S., Yang, C., Chen, A., 2005. Shelter location-allocation model for flood evacuation planning. J. East. Asia Soc. Transp. Stud.
Langmann, B., Folch, A., Hensch, M., Matthias, V., 2012. Volcanic ash over Europe during the eruption of Eyjafjallajökull on Iceland, April-May 2010. Atmos. Environ. 48, 1–8. https://doi.org/10.1016/j.atmosenv.2011.03.054.
Lin, Y.H., Batta, R., Rogerson, P.A., Blatt, A., Flanigan, M., 2012. Location of temporary depots to facilitate relief operations after an earthquake. Socioecon. Plann. Sci. 46, 112–123. https://doi.org/10.1016/j.seps.2012.01.001.
Liu, S.Q., Kozan, E., 2016. Parallel-identical-machine job-shop scheduling with different stage-dependent buffering requirements. Comput. Oper. Res. 74, 31–41. https://doi.org/10.1016/j.cor.2016.04.023.
Lordan, O., Klophaus, R., 2017. Measuring the vulnerability of global airline alliances to member exits. Transp. Res. Procedia 25, 7–16. https://doi.org/10.1016/j.trpro.2017.05.189.
Lordan, O., Sallan, J.M., Simo, P., 2014. Study of the topology and robustness of airline route networks from the complex network approach: a survey and research agenda. J. Transp. Geogr. 37, 112–120. https://doi.org/10.1016/j.jtrangeo.2014.04.015.
Lordan, O., Sallan, J.M., Simo, P., Gonzalez-Prieto, D., 2015. Robustness of airline alliance route networks. Commun. Nonlinear Sci. Numer. Simul. 22, 587–595. https://doi.org/10.1016/j.cnsns.2014.07.019.
Madas, M.A., Zografos, K.G., 2010. Airport slot allocation: a time for change? Transp. Policy 17, 274–285. https://doi.org/10.1016/j.tranpol.2010.02.002.
Marinelli, M., Palmisano, G., Dell'Orco, M., Ottomanelli, M., 2015. Fusion of two metaheuristic approaches to solve the flight gate assignment problem. Transp. Res. Procedia 10, 920–930. https://doi.org/10.1016/j.trpro.2015.09.045.
Mazzocchi, M., Hansstein, F., Ragona, M., 2010. The 2010 volcanic ash cloud and its financial impact on the European airline industry. CESifo Forum.
MLIT, 2018. Collaborative Actions for Renovation of Air Traffic Systems (CARATS) [WWW Document]. Minist. land, Infrastruct. Transp. URL http://www.mlit.go.jp/common/001046514.pdf (accessed 6.1.19).
Mota, M.M., Boosten, G., De Bock, N., Jimenez, E., de Sousa, J.P., 2017. Simulation-based turnaround evaluation for Lelystad Airport. J. Air Transp. Manag. 64, 21–32. https://doi.org/10.1016/j.jairtraman.2017.06.021.
NRT, 2020. Flight Information | NARITA INTERNATIONAL AIRPORT OFFICIAL WEBSITE [WWW Document]. accessed 2.12.20. https://www.narita-airport.jp/en/flight/today#section-1.
Picquout, A., Lavigne, F., Mei, E.T.W., Grancher, D., Noer, C., Vidal, C.M., Hadmoko, D.S., 2013. Air traffic disturbance due to the 2010 Merapi volcano eruption. J. Volcanol. Geotherm. Res. 261, 366–375. https://doi.org/10.1016/j.jvolgeores.2013.04.005.
Poulidis, A.P., Takemi, T., Shimizu, A., Iguchi, M., Jenkins, S.F., 2018. Statistical analysis of dispersal and deposition patterns of volcanic emissions from Mt. Sakurajima. Japan. Atmos. Environ. 179, 305–320. https://doi.org/10.1016/j.atmosenv.2018.02.021.
Smith, I.E., Arnedos, M., 2007. The evolution of adjuvant endocrine therapy: developments since St Gallen 2005. Breast 16, 4–9. https://doi.org/10.1016/j.breast.2007.07.001.
Smith, J.F., 2010. Regional cooperation, coordination, and communication between airports during disasters. Transp. Res. Rec. J. Transp. Res. Board 2177, 132–140. https://doi.org/10.3141/2177-16.
Toregas, C., Swain, R., ReVelle, C., Bergman, L., 1971. The location of emergency service facilities. Oper. Res. https://doi.org/10.1287/opre.19.6.1363.